ACOUSTIC EMISSION OF BOLT-BEARING TESTING ON STRUCTURAL COMPOSITE LUMBERS

Yicheng Du

Postdoctoral Fellow
University of Toronto
Toronto, Ontario, Canada M5S 3B3
E-mail: yicheng.du@utoronto.ca

*Jilei Zhang**

Professor
Department of Forest Products
Mississippi State University
Mississippi State, MS 39762-9820
E-mail: jzhang@cfr.msstate.edu

Sheldon Shi†

Associate Professor
Department of Mechanical and Energy Engineering
University of North Texas
Denton, TX 76207-7102
E-mail: Sheldon.shi@unt.edu

(Received June 2013)

Abstract. Acoustic emission (AE) characteristics of full-hole bolt-bearing testing on structural composite lumbers (SCL) including laminated veneer lumber (LVL) and oriented strand lumber (OSL) were investigated. The main conclusion is that AE cumulative counts vs time curves of the tested SCL in this study can be characterized with three distinct regions in terms of AE count rates: Region I with a lower constant count rate, Region II with varied and increased count rates, and Region III with a higher constant count rate. Differences in AE count rates of these three regions occurred between LVL and OSL. Also, within each tested SCL, differences in AE count rates were observed among the three regions. These differences in terms of AE count rates between two tested SCL indicate that different types of wood-based composites might have different AE characteristics in terms of the count rate changes when they are subjected to increased bolt compression load. In other words, these differences in AE characteristics between the two tested materials suggest AE "signatures" do exist for SCL bolt connections.

Keywords: Acoustic emission (AE), structural composite lumbers, bolted connection, cumulative AE counts, AE count rate, AE signature, bolt-bearing strength.

INTRODUCTION

Bolted connections have been widely used in heavy timber and structural composite lumber (SCL) constructions. The design practice for bolted connections in the US is based on the yield theory developed by Johanson (1949) because this theory adequately describes single-bolt connections (Soltis 1994). The nominal design value, Z, in National Design Specification (NDS) for Wood Construction (AF&PA 2001) is affected by main and side connection member dowel-bearing strengths, F_e, for parallel- or perpendicular-to-grain loading. Dowel-bearing strengths provided in NDS for wood members can be determined in accordance with ASTM (2004b). Dowel-bearing strength is defined as yield load obtained from the load-deformation curve of a dowel-bearing test divided by dowel

* Corresponding author
† SWST member

diameter and specimen thickness. The bearing yield load of a tested specimen is determined through fitting a straight line to the initial linear portion of the load-deformation curve recorded during the test, offsetting this line by a deformation equal to 5% of the bolt diameter, and finally selecting the load at which the offset line intersects the load-deformation curve.

Acoustic emission (AE) is defined as the class of phenomena in which transient elastic waves are generated by the rapid release of energy from a localized source or sources within a material (ASTM 2002). All materials, including SCL, contain minute flaws randomly distributed throughout their volume. Subjected to stress, these flaws initiate microfractures. As the stress increases, the microfractures randomly enlarge in intermittent step-like bursts. During each burst, high-frequency soundwaves are produced (Knuffel 1988). These elastic waves can be detected by resonant transducers. Therefore, the AE method allows observation and registration of destructive changes occurring in a material at the moment of stress. It provides possibilities to follow destructive processes that take place in bolt connections, beginning with microcracks and ending up in total failure.

Many AE techniques can be used to locate and characterize the source by using different parameters that characterize an AE signal. Those parameters (Bucur 1995) are mode of emission (continuous or burst); rate of emission; the acoustic emission event (Beall and Wilcox 1987); the accumulated activity, total number of events observed during a specific period of time (Aicher et al 2001); the threshold set at a selected discriminator level; duration of the event; AE cumulative count (Porter et al 1972; Ansell 1982; Sato et al 1984; Noguchi et al 1992; Raczkowski et al 1999; Ayarkwa et al 2001; Gozdecki and Smardzewski 2005; Ando et al 2006; Chen et al 2006; Ritschel et al 2013); AE count rates (Sato et al 1984; Gozdecki and Smardzewski 2005; Smardzewski and Gozdecki 2007); AE cumulative energy (Knuffel 1988; Ritschel et al 2013); and average AE energy (Ritschel et al 2013).

AE signals generated during a bolt-bearing test on SCL provided important information about all destructive processes occurring and changes taking place in the material from which they are emitted (Porter et al 1972). These acoustic emissions are caused by localized failure of the wood or wood-based material (Beall and Wilcox 1987). Two types of localized wood failure modes commonly occur at connections subjected to lateral compression loads: crushing of wood fibers in the bearing adjacent to the bolt and splitting of wood fibers. Each of these types of failures might generate unique acoustic signatures.

AE is a popular nondestructive material testing technique because it gives information regarding plastic deformation and failure of materials (Ayarkwa et al 2001). Therefore, if appropriate characteristics of AE signals generated from bolt-bearing test specimens constructed with assorted SCL can be identified with "signatures," then AE information would be used to develop a nondestructive evaluation (NDE) monitoring of damage occurring in bolt connections in terms of identifying different stages of material fracture: initiation, propagation, and destruction (Porter et al 1972; Knuffel 1988).

Limited literature was found that used AE to characterize the compressive load-bearing behavior of bolted connections in wood-based SCL such as laminated veneer lumber (LVL) and oriented strand lumber (OSL) with quantitative analyses of AE count rates for each of three crack development regions, initiation, propagation, and catastrophic failure. Therefore, the main objectives of this investigation were to study AE signal characteristics of bolt-bearing behavior in selected SCL and to characterize compressive load-bearing behaviors of bolted connections using AE techniques.

MATERIALS AND METHODS

Experimental Design

Figure 1 shows the configuration of a bolt-bearing strength test specimen used in this study by referencing ASTM (2004a, 2004b). The specimen

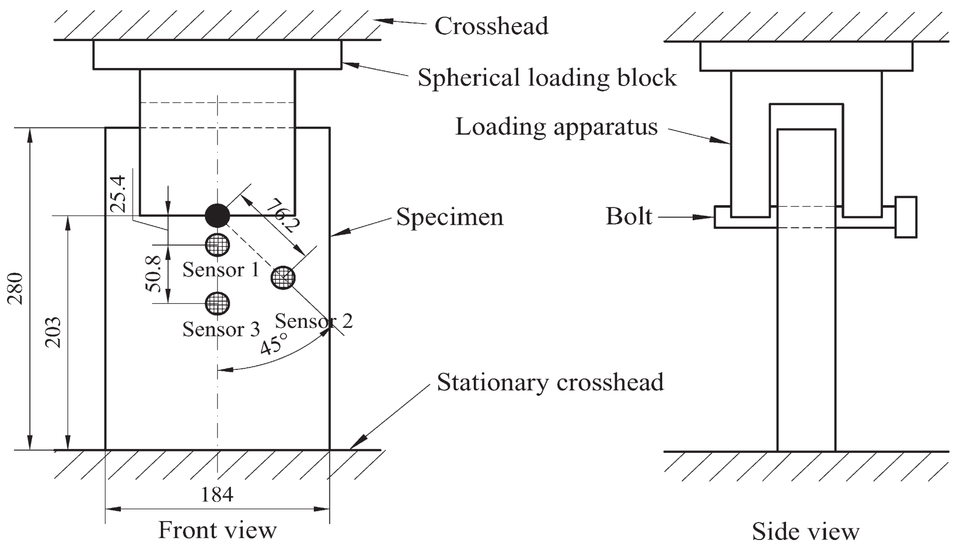

Figure 1. Schematic of full-hole bolt-bearing testing specimen and setup.

measured 184 mm wide × 279 mm tall. Grade 5 19.1-mm-diameter bolts were used for the evaluation. The holes for the bolts in the specimens were drilled 1.59 mm larger than the bolt diameter. The loaded length was 203 mm.

Experiments with a complete two × two factorial design with five replications per cell were conducted to evaluate loading capacity and AE characteristics of bolted connections in SCL subjected to compression loads. Factors investigated were material type (LVL, OSL) and loading direction (parallel and perpendicular to material surface veneer or strand orientation). LVL specimens were supplied from International Paper (Thorsby, AL) and were 41.3 mm thick. OSL specimens used in this study were commercial APA Rimboard Plus supplied by Grant Forest Products (Fairfax, SC). OSL was 28.6 mm thick. The wood species of the two evaluated materials was southern pine.

Acoustic Emission Apparatus

The AE apparatus used in this experiment consisted of an AE measuring system box called DiSP (Digital Signal Process), a laptop computer with Physical Acoustics Corporation (PAC) AEwin (Acoustic Emission for Windows) installed, and PAC acoustic emission sensors. AEwin is a software program that takes the data from DiSP, records it in terms of AE events and AE counts, and represents it in graphical form. The AE sensor operating frequency range was from 50 to 200 kHz. For wood-based materials, the range of about 100-200 kHz provided sufficient sensitivity to emissions of interest (Beall 1985).

Testing

Figure 1 shows a schematic diagram of the testing setup for the full-hole bolt-bearing test. There were three sensors mounted by silicon grease on each specimen. Sensor 1 was placed on the specimen surface 25.4 mm beneath the center of the bolt. Sensor 2 was 76.2 mm diagonally to the right and left of the bolt. Sensor 3 was 76.2 mm below the bolt. This study only reports results from AE activities recorded on Sensor 1.

All tests were performed on a Tinius–Olsen universal testing machine according to ASTM (2004b) at a loading rate of 1 mm/min. Load-deformation curves with synchronous AE activities were recorded. The threshold was set at 30 dB, and the preamp was set at 40 dB. A filter was set at a range from 10 to 100 kHz. Prior to bearing testing, all specimens were conditioned in a 12% RH chamber.

RESULTS AND DISCUSSION

Figures 2 and 3 show synchronous parts of typical cumulative counts vs time and load vs deformation curves of each of the four tested groups, LVL specimens loaded parallel and perpendicular to grain, and OSL specimens loaded parallel and perpendicular to grain. Specific gravity of LVL and OSL averaged 0.53 and 0.54, respectively. Moisture content of LVL and OSL averaged 10.1 and 10.5%, respectively. Mode of failure observed was mainly crushing of the wood under the bolt.

Table 1 summarizes mean stresses corresponding to different critical load points on the load-deformation curve for each of the four tested specimen groups. Table 2 summarizes mean AE count rates for Regions I and III of each tested specimen group. Table 3 summarizes the ratios of each stress at different load points on load-deformation curves to its corresponding stress at the proportional limit for each of the four tested specimen groups.

Load-deformation Curves

The interpretation of results of load-deformation curves such as proportional limit load, P_{pl}, yield load, P_y, and ultimate load, P_u, was referenced to ASTM (2004b). The proportional limit load (Fig 2a) is the load at which the load-deformation curve deviates from a straight line fitted to the initial linear portion of the load-deformation curve. The yield load is determined by offsetting the straight line by a deformation equal to 5% of the bolt diameter and selecting the load at which the offset line intersects the load-deformation curve. The bolt-bearing stress at a point on the load-deformation curve is calculated by dividing the load at the point by the bolt diameter and specimen thickness.

In general, the bolt-bearing strength of both LVL and OSL loaded parallel to specimen surface grain direction is higher than those loaded in the perpendicular direction (Table 1). The average yield strength of the specimens loaded parallel to their surface grain directions is 1.39 and 1.20 times the ones loaded perpendicular for LVL and OSL, respectively.

The ultimate bolt-bearing strength is close to the yield strength (Table 1), except for LVL loaded in the perpendicular direction, for which the ultimate bolt-bearing strength is higher than yield strength. For LVL and OSL loaded parallel (Figs 2a and 3a), yield and ultimate loads were very close, but yield loads tended to be reached first. For OSL loaded in the perpendicular direction (Fig 3b), the maximum yield load tended to be reached first. The yield load was reached first for all LVL specimens loaded in the perpendicular direction (Fig 2b).

Cumulative Acoustic Emission Counts-Time Curves

In general, the cumulative AE counts-time curves (Figs 2 and 3) show that the AE count rate (the slope of the curve) starts off with a low and constant value, gradually increasing to a point at which the rate becomes a constant value again. Based on this observation, three distinct stages of cumulative counts were identified regarding curve slope changes: initiation, growth, and acceleration (Raczkowski and Molinski 1994) (Fig 2a). Initiation stage (Region I) is the first linear portion in which the AE count rate is lower and constant. This is because the fracture can take place on a microscopic scale at the stress level well below the proportional limit (Bodig and Jayne 1982). These microscopic failures can be detected using an AE device (DeBaise et al 1966). Growth stage (Region II) is the second curve portion showing the increase of AE count rate in which the acoustic activity grows gradually (Raczkowski and Molinski 1994). In this region, cracks developed and propagated as the applied load increased (Bodig and Jayne 1982).

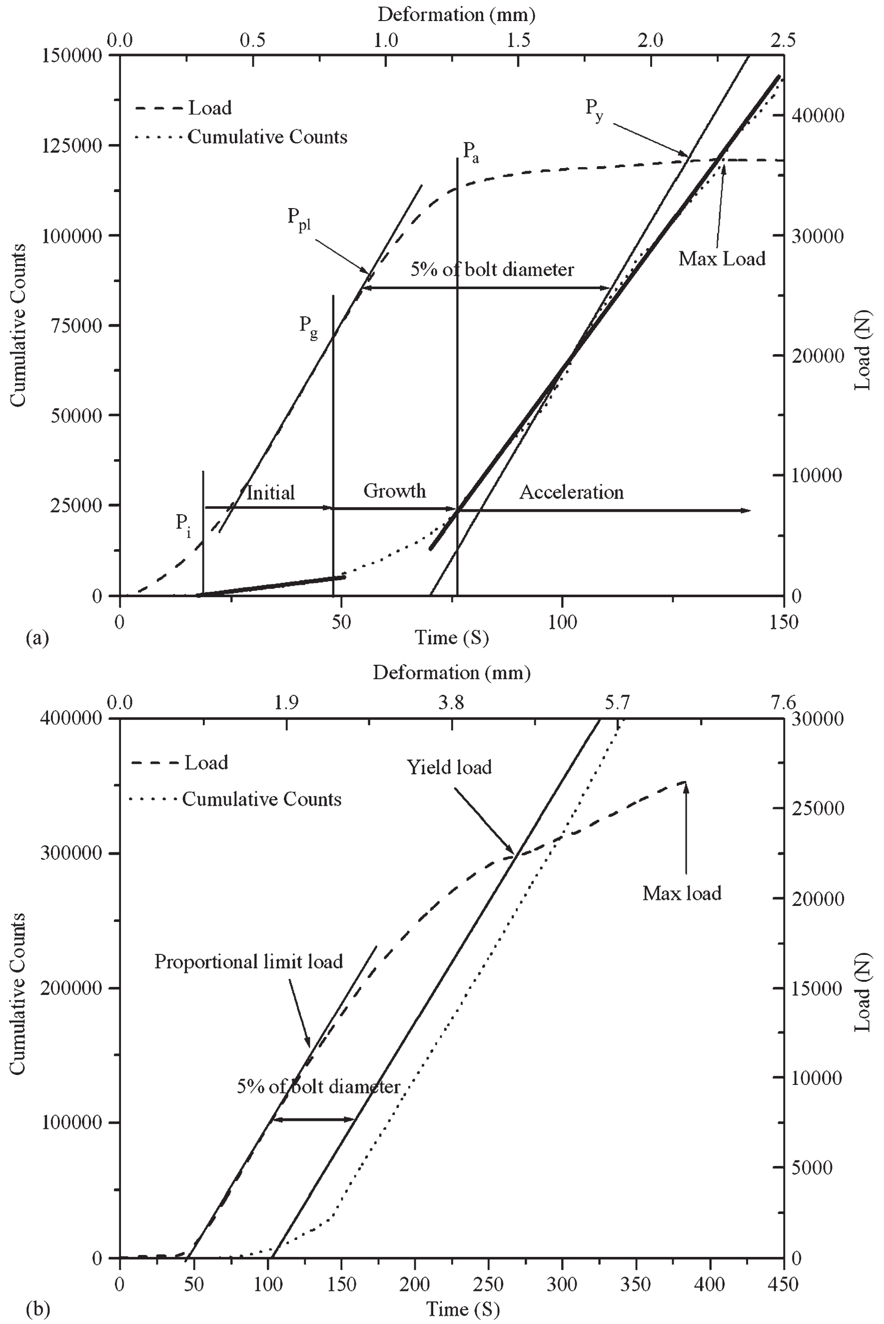

Figure 2. Typical cumulative counts-time and load-deformation curves showing acoustic emission behavior of full-hole bolt-bearing testing on laminated veneer lumber (a) parallel and (b) perpendicular to surface veneer orientation.

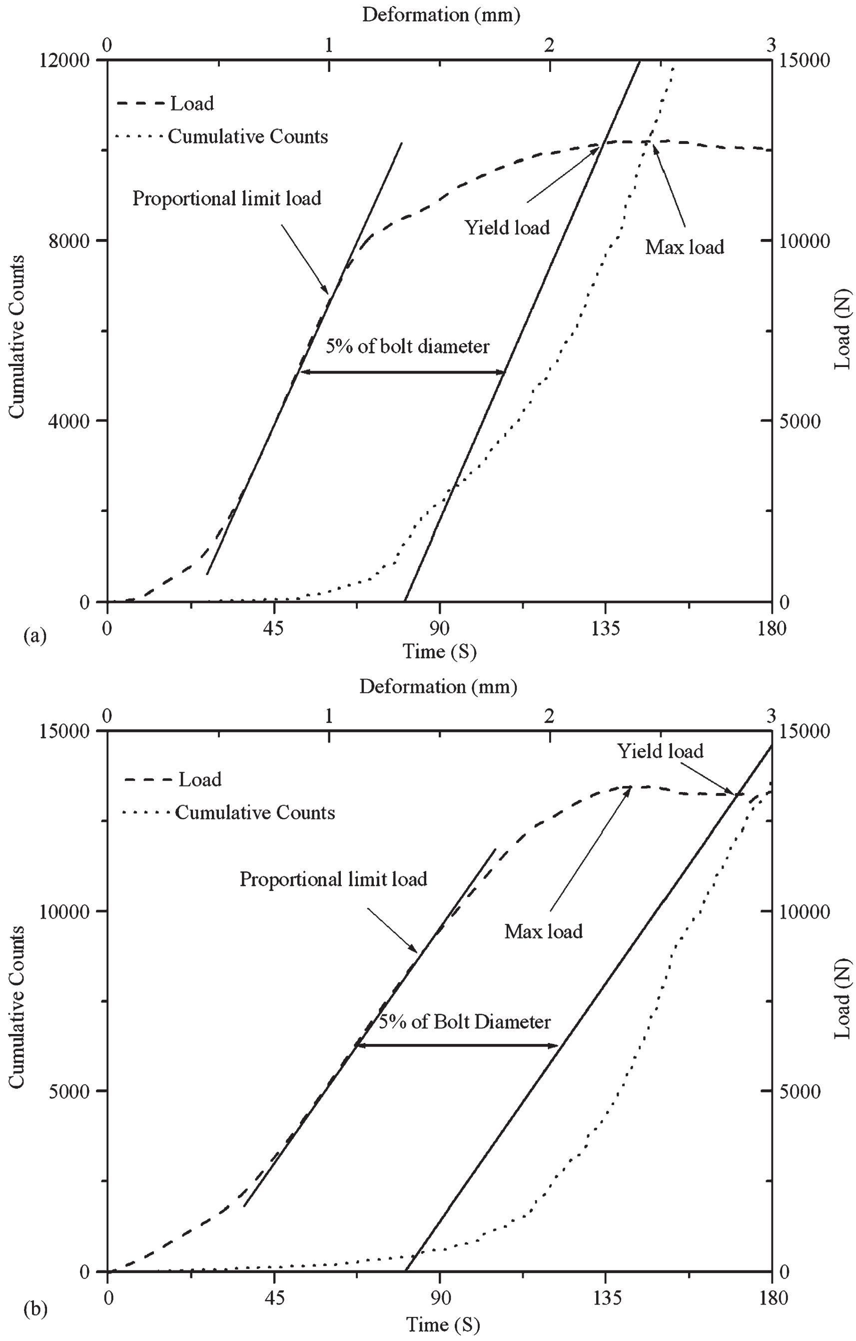

Figure 3. Typical cumulative counts-time and load-deformation curves showing acoustic emission behavior of full-hole bolt-bearing testing on oriented strand lumber (a) parallel and (b) perpendicular to surface strand orientation.

Table 1. Mean stress values corresponding to different critical load points on the load-deformation curve for each of four tested specimen groups.

Material type	Loading direction	P_i (kPa)	P_g (kPa)	P_{pl} (kPa)	P_a (kPa)	P_y (kPa)	P_u (kPa)
LVL	Parallel	1650 (45)[a]	20,500 (36)	30,000 (12)	36,900 (17)	43,200 (6)	43,300 (6)
	Perpendicular	1370 (38)	8780 (10)	12,800 (15)	16,100 (10)	31,000 (8)	34,800 (6)
OSL	Parallel	3940 (63)	21,000 (6)	18,000 (17)	27,000 (9)	26,700 (8)	27,100 (8)
	Perpendicular	4070 (53)	14,900 (30)	15,600 (24)	20,600 (21)	22,300 (10)	22,600 (10)

[a] Values in parentheses are coefficients of variation in percent.
LVL, laminated veneer lumber; OSL, oriented strand lumber.

Therefore, the growth stage can be viewed as a transitional progressive region between Regions I and III in which the AE count rate increased from low to high. Acceleration stage (Region III) is the third portion in which the AE count rate remained high and constant up to specimen failure at which the acoustic activity reached exponential increase (Raczkowski and Molinski 1994). In this region, the cracks grew further, their resistance to stresses became low, and the cracks accelerated and catastrophic failure resulted. This accelerated crack growth yielded more AE activities.

Regression analyses of each individual AE cumulative counts-time curve of tested specimens showed that a strong linear relationship existed between cumulative AE counts and time within Regions I and III. The mean values of coefficients of determination (r^2) of those lines ranged from 0.843 to 0.997 with coefficients of variation ranging from 0.2 to 7.7% (Table 2). Therefore, the slopes of simple linear functions were calculated for each data set, ie two slopes were obtained for two linear regions.

Table 2 summarized the mean values of calculated slopes (AE count rates) for the two linear portions of each combination of material type × loading direction. The averaged AE count rates for LVL in Region I were 56 and 43 counts/s for parallel and perpendicular loading directions, respectively, and there was little difference between the two rates. These two rates are much lower than their corresponding rates in Region III, which were 531 and 1104 counts/s for parallel and perpendicular loading directions, respectively. In Region III, the AE count rate of LVL loaded in perpendicular direction is almost twice that of the one in parallel direction. A similar trend of higher AE count rates in Region III compared with Region I was observed for OSL (Table 2). However, there was not much difference between the two rates in Region III of OSL. In general, OSL specimens subjected to bolt-bearing load have much lower AE count rates than LVL.

Average bolt-bearing stresses corresponding to loads, P_i, P_g, and P_a, at three points along load-deformation curves (Fig 2a) for each tested

Table 2. Summary of mean acoustic emission counts rate values for Regions I and III of each of four tested specimen groups.

		Region			
		I		III	
Material type	Grain orientation	Rate (counts/s)	r^2	Rate (counts/s)	r^2
LVL	Parallel	56 (110)[a]	0.959 (2.2)	570 (56)	0.987 (0.5)
	Perpendicular	43 (81)	0.911 (2.7)	1104 (66)	0.997 (0.2)
OSL	Parallel	4 (29)	0.843 (4.7)	193 (7)	0.994 (0.6)
	Perpendicular	11 (71)	0.896 (7.7)	203 (23)	0.995 (0.4)

[a] Values in parentheses are coefficients of variation in percent.
LVL, laminated veneer lumber; OSL, oriented strand lumber.

Table 3. Summary of load ratios of each load to its corresponding load at proportional limit for each of four tested groups.

Material type	Loading direction	P_i	P_g	P_{pl}	P_a	P_y
LVL	Parallel	0.06	0.68	1	1.23	1.44
	Perpendicular	0.11	0.69	1	1.26	2.42
OSL	Parallel	0.22	1.17	1	1.50	1.48
	Perpendicular	0.26	0.96	1	1.32	1.43

LVL, laminated veneer lumber; OSL, oriented strand lumber.

group were calculated and summarized in Table 1. P_i is the load on a load-deformation curve corresponding to a point on the cumulative counts-time curve at which Region I starts with the first AE activity. P_g is the load corresponding to a point on the cumulative counts-time curve at which Region I ends and Region II starts. P_a is the load corresponding to a point on the cumulative counts-time curve at which Region II ends and Region III starts.

For LVL loaded parallel (Table 1), no AE activity was recorded prior to the compression stress reaching 1650 kPa, which is 6% of its stress at a proportional limit (Table 3). For LVL loaded perpendicular, AE activities began at a stress of 1370 kPa, which is 11% of its stress at a proportional limit. For OSL, the two stress values are 3940 and 4070 kPa for parallel and perpendicular loads, respectively, which are 22 and 26% of their stresses at proportional limits, respectively.

Table 3 indicates that the load, P_g, was 0.68 and 0.69 times that of P_{pl} for LVL materials loaded parallel and perpendicular, respectively. This implies that the material underneath the bolt still could have been in the elastic range when the measured AE count rate was in the 50-counts/s range (Table 2). The load, P_a, of LVL loaded parallel was 1.23 times that of P_{pl} and the load, P_y, was 1.44 times that of P_{pl} (Table 3). This implies that once the measured AE count rate reached 570 counts/s, the stress of LVL underneath the bolt might have been beyond its proportional limit and approaching 5% of the yield failure point. The load, P_a, of LVL loaded perpendicular was 1.26 times that of P_{pl}, and the load, P_y, was 2.42 times that of P_{PL}. This might imply that once the average AE count rate reached 1104 counts/s, the stress of LVL material underneath the bolt may have exceeded its proportional limit and started to approach failure but may still have been far from 5% of the yield failure point.

In the case of OSL subjected to load parallel to grain (Table 3), the load, P_g, was 1.17 times that of P_{pl}. This means that there is a possibility that the loaded material underneath the bolt could have had some permanent damage that occurred in Region I. The load, P_a, was 1.50 times that of P_{pl} (Table 3), and the load, P_y, was 1.48 times that of P_{pl}. This means a measured AE count rate of 193 counts/s would indicate that the stress of OSL material underneath the bolt reached the 5% yield point.

For the OSL loaded perpendicular, the load, P_g, was 0.96 times that of P_{pl}, whereas the load, P_a, was 1.32 times that of P_{pl}, and the yield load, P_y, was 1.43 times that of P_{pl}. This result indicated that the loaded material underneath the bolt was still in the elastic range in Region I if an averaged AE count rate of 11 counts/s was measured. Once the measured AE count rate reached 203 counts/s, the stress of the OSL material underneath the bolt may have been beyond its proportional limit and approaching the 5% yield failure point.

CONCLUSIONS

AE characteristics of full-hole bolt-bearing testing on SCL were investigated through analyzing AE cumulative counts vs time curves and synchronously recorded load-deformation curves from tested LVL and OSL specimens. In general, the AE cumulative counts vs time curves of tested SCL can be characterized with three distinct regions in terms of AE count rates, Region I with lower constant count rate, Region II with varied and increased count rate, and

Region III with higher constant count rate. Differences in the AE count rate of these three regions occurred between LVL and OSL. Also, within each tested material, differences in AE count rates occurred among three regions.

These differences in terms of AE count rates between two SCL (LVL and OSL) suggest that different types of wood-based composites have different AE characteristics in terms of count rate changes when they are subjected to increased bolt compression stresses. In other words, these differences in AE cumulative counts-time curves observed in this study might suggest that AE "signatures" do exist for SCL bolted connections. This information might be used to develop an NDE device to detect damage progress of bolted connections in a structure.

ACKNOWLEDGMENTS

Special thanks to International Paper Company and Grant Forest Products Company who supplied materials for this study. Approved for publication as Journal Article No. FP 485 of the Forest and Wildlife Research Center, Mississippi State University.

REFERENCES

AF&PA (2001) National design specification (NDS) for wood construction. American Forest & Paper Association, Washington, DC.

Aicher S, Hofflin L, Dill-Langer G (2001) Damage evolution and acoustic emission of wood at tension perpendicular to fiber. Holz Roh Werkst 59:104-116.

Ando K, Hirashima Y, Sugihara M (2006) Microscopic processes of shearing fracture of old wood, examined using the acoustic emission technique. J Wood Sci 52:483-489.

Ansell MP (1982) Acoustic emission from softwood in tension. Wood Sci Technol 16:35-58.

ASTM (2002) E 1316. Standard terminology for nondestructive examinations. American Society for Testing and Materials, West Conshohocken, PA.

ASTM (2004a) D 5456-99a. Standard specification for evaluation of structural composite lumber products. American Society for Testing and Materials, West Conshohocken, PA.

ASTM (2004b) D 5764-97a. Standard test method for evaluating dowel-bearing strength of wood and wood-based products. American Society for Testing and Materials, West Conshohocken, PA.

Ayarkwa J, Hirashima Y, Ando K, Sasaki Y (2001) Monitoring acoustic emissions to predict modulus of rupture of finger-joints from tropical African hardwoods. Wood Fiber Sci 33(3):450-464.

Beall FC (1985) Relationship of acoustic emission to internal bond strength of wood-based composite panel materials. J Acoustic Emission 4(1):19-29.

Beall FC, Wilcox WW (1987) Relationship of acoustic emission during radial compression to mass loss from decay. Forest Prod J 37(4):38-42.

Bodig J, Jayne BA (1982) Mechanics of wood and wood composites. Van Nostrand Reinhold Company Inc., New York, NY. 712 pp.

Bucur V (1995) Acoustics of wood. CRC Press, Inc., Boca Raton, FL.

Chen Z, Gabbita B, Hunt D (2006) Monitoring the fracture of wood in torsion using acoustic emission. J Mater Sci 41:3645-3655.

DeBaise G, Porter A, Pentoney R (1966) Morphology and mechanics of wood fracture. Materials Research and Standards 6(10):493-499.

Gozdecki C, Smardzewski J (2005) Detection of failures of adhesively bonded joints using the acoustic emission method. Holzforschung 59:219-229.

Johanson KW (1949) Theory of timber connections. International Association for Bridge and Structural Engineering 9:249-262.

Knuffel WE (1988) Acoustic emission as strength predictor in structural timber. Holzforschung 42:195-198.

Noguchi M, Ishii R, Fujii Y, Imamura Y (1992) Acoustic emission monitoring during partial compression to detect early stages of decay. Wood Sci Technol 26:279-287.

Porter AW, El-Osta ML, Kusec DJ (1972) Prediction of failure of finger joints using acoustic emission. Forest Prod J 22:74-82.

Raczkowski J, Lutomski K, Molinski W, Wos R (1999) Detection of early stages of wood decay by acoustic emission technique. Wood Sci Technol 33:353-358.

Raczkowski J, Molinski W (1994) Acoustic emission in fracture mechanics of wood. J Theor Appl Mech 2(32): 300-322.

Ritschel F, Brunner AJ, Niemz P (2013) Nondestructive evaluation of damage accumulation in tensile test specimens made from solid wood and layered wood materials. Compos Struct 95:44-52.

Sato K, Fushitani M, Noguchi M (1984) Discussion of tensile fracture of wood using acoustic emissions—Estimation of tensile strength and consideration of AE generation based on fracture mechanics. J Japan Wood Res Soc 30(2):117-123.

Smardzewski J, Gozdecki C (2007) Decohesion of glue bonds in wood connections. Holzforschung 61:291-293.

Soltis LA (1994) Bolted connection research: Present and future. Wood Design Focus 5(2):3-5.